Nanoscale

Volume 1 | Number 1 | Jan 2013 | Pages 1–100

Nanoscale

www.rsc.org/nanoscale

ROYAL SOCIETY OF CHEMISTRY

ROYAL SOCIETY OF CHEMISTRY

www.rsc.org/nanoscale

Intrinsic polarization control in rectangular GaN nanowire lasers

Changyi Li[1], Sheng Liu[2,3], Ting. S. Luk[2,3], Jeffrey J. Figiel[2], Igal Brener[2,3], S. R. J. Brueck[1], George T. Wang[2*]

[1] Center for High Technology Materials, University of New Mexico, 1313 Goddard St. SE, Albuquerque, NM, 87106, USA.

[2] Sandia National Laboratories, Albuquerque, New Mexico 87185, USA.

[3] Center for Integrated Nanotechnology, Sandia National Laboratories, Albuquerque, New Mexico 87185, USA.

*Author to whom correspondence should be addressed: gtwang@sandia.gov

ABSTRACT: We demonstrate intrinsic, linearly polarized lasing from single GaN nanowires using cross-sectional shape control. A two-step top-down fabrication approach was employed to create straight nanowires with controllable rectangular cross-sections. A clear lasing threshold of 444kW/cm^2 and a narrow spectral linewidth of 0.16 nm were observed under optical pumping at room temperature, indicating the onset of lasing. The polarization was along the short dimension (y-direction) of the nanowire due to the higher transverse confinement factors for y-polarized transverse modes resulting from the rectangular nanowire cross-section. The results show that cross-sectioned shape control can enable inherent control over the polarization of nanowire lasers without additional environment requirements, such as placement onto lossy substrates.

KEYWORDS: rectangular, nanowire, laser, GaN, polarization

Introduction

Semiconductor nanowire lasers have drawn significant attention as potential compact and low power coherent light sources for extensive applications, including on-chip integrated photonic circuits[1], high speed communication[2], and sensing[3]. In order to improve the performance and broaden the applications, control over the fundamental lasing properties of semiconductor nanowire lasers has been reported by multiple groups. For example, single mode lasing has been demonstrated using dimension control[4], coupled nanowire laser pairs[5,6], folded nanowire lasers[7], distributed feedback lasers[8] and integration with a lossy gold substrate[9]. Wavelength selection has been reported using InGaN/GaN nanowire photonic crystal arrays[10,11], compositionally graded nanowire ensembles[12,13], bandgap graded nanowires[14], self-absorption of nanowires[15], Surface plasmon polariton enhanced Burstein-Moss effect[16], and dynamic wavelength tuning was reported via applied hydrostatic pressure on single GaN nanowire lasers[17]. Annular shaped emission was also reported by using a hollow GaN nanotube laser geometry, showing the possibility of beam shaping via cross-sectional shape control[18].

In addition to control of the above optical properties, polarization control is also critical for applications, such as optical communication[19,20], non-linear optics[21], and compact laser-based displays. However, due to their nanoscale size, polarization control in nanowire lasers has been challenging. Recently, linearly polarized, single mode emission from single GaN

nanowire lasers was demonstrated by placing GaN nanowire lasers onto a gold substrate[22], which induces mode-dependent losses. Nevertheless, the gold substrate results in undesired higher propagation losses and therefore higher lasing thresholds. More importantly, requiring the nanowire laser to be placed onto a gold or other lossy substrate limits the flexibility with which the nanowire can be placed and integrated into any given application or device.

Linearly polarized *spontaneous* emission along the elongated nanowire axis has been recently demonstrated from embedded InAs[23] and InGaAs[24] quantum dots in GaAs nanowires with elliptical cross-sections. Here, we extend this concept to control the polarization of nanowire lasers (i.e. stimulated emission instead of spontaneous emission) for the first time. Using a top-down approach, we demonstrate GaN nanowires with unique, rectangular cross-sections which exhibit *intrinsic*, linearly polarized lasing under optical pumping without the need for a lossy substrate or other environmental requirements[22].

Fabrication of rectangular cross-sectioned GaN nanowire lasers

The GaN rectangular nanowire lasers were fabricated by a top-down two-step dry plus wet etch process that was previously developed to fabricate straight and smooth quasi-cylindrical GaN nanowires[4,17,25] (Figure 1(a-c)). An unintentionally doped ~4 μm thick *c*-plane (0001) GaN epitaxial film was first grown on a 2 inch *c*-plane sapphire wafer by metal organic chemical vapor deposition. Electron beam lithography was employed on the GaN film, using a 495 polymethyl methacrylate (PMMA) C6 resist to define rectangular-shaped nickel dots as a dry etch mask. The rectangular Ni pattern was subsequently transferred into the GaN film by a chlorine-based inductively coupled plasma (ICP) dry etch. Following the dry etch

process, a KOH based (AZ400K developer) crystallographically selective wet etching was employed to remove the sidewall roughness and the dry etch damage, resulting in GaN nanowires with straight, vertical, and smooth sidewalls and rectangular cross-sections. As seen in the SEM image (Figure 1(d) and 1(e)), the rectangular cross-sectioned GaN nanowires (Sample A) have x-dimensions of ~450 nm, y-dimensions of ~120 nm and heights of ~4 μm. The corners are slightly rounded due to the limitation of the etch process. Another nanowire sample (sample B) was also fabricated to study the effect of varying the y-dimension on the polarization of the emission. The nanowires from Sample B have larger y-dimensions (~300 nm), the same x-dimension, and the same height as the nanowires from Sample A.
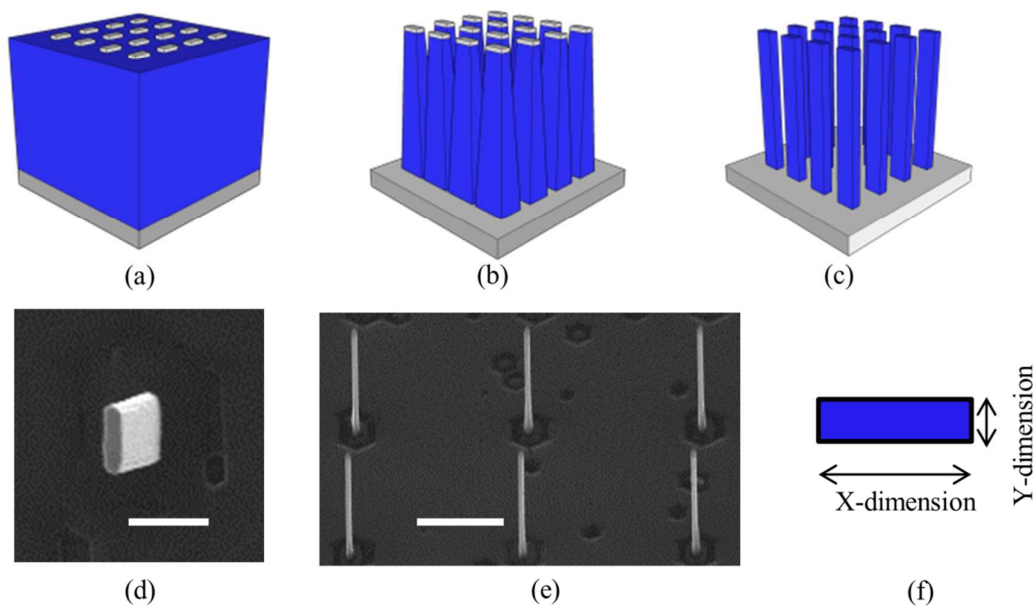
Figure 1. Schematic of the fabrication process and SEM images of rectangular GaN nanowire lasers. (a) Rectangular Ni patterns were deposited by e-beam patterning on top of a planar GaN film. (b) The rectangular patterns were transferred into the GaN film using ICP etching, resulting in tapered pillars. (c) GaN nanowires with smooth and vertical sidewalls

are formed using a KOH-based wet etch process. (d) Plan-view SEM image of resulting rectangular GaN nanowires, scale bar: 500 nm. (e) 45° view SEM image of rectangular GaN nanowires from. Scale bar: 2.5µm. (f) Diagram indicating long x- and short y-axes.

Optical characterization and numerical simulation of the rectangular GaN nanowire lasers

The optical properties of the rectangular cross-sectioned GaN nanowire lasers were characterized by a custom 2-arm micro-photoluminescence (µ-PL) experimental setup described in previous papers[22,26]. In the pumping arm, a 50X infinity-corrected objective was employed to focus the pump laser beam, a pulsed 266nm frequency quadrupled Nd:YAG laser with a pulse width of 400 ps, to a 3.5 µm diameter spot on the as-fabricated GaN nanowire sample. The center-to-center distance of the as-fabricated GaN nanowires was designed to be 5 µm, allowing for pumping individual devices. For the lasing threshold measurement, a series of neutral density filters was used to vary the pump power density. The emission from a rectangular cross-sectioned GaN nanowire laser was collected by the same objective and focused to an optical fiber, which then transmitted the emission to a multimode optical detection fiber-coupled, 2400 groove/mm holographic grating spectrometer. In order to measure the polarization of the emission, the nanowires were transferred to hang off the edge of a sapphire or silicon substrate using a cotton swab (Figure 3(a)), to minimize the effects of reflection from the substrate surface. The end-facet emission from the GaN nanowires was collected by another 40× objective in the collection arm. A motor-driven, high-extinction ratio polarizer was placed between the objective and an optical fiber to measure the polarization properties of the emission.
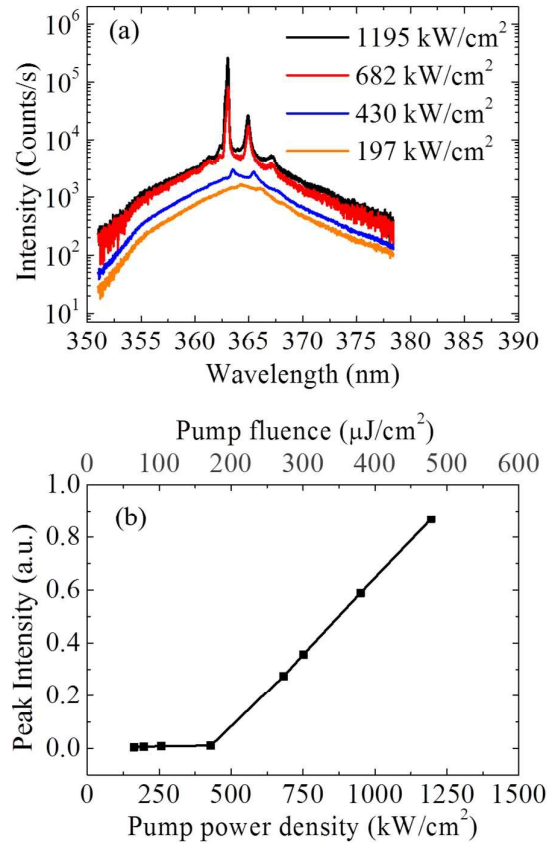
Figure 2. (a) Room temperature μ-PL spectra of the emission from an as-fabricated Sample A GaN nanowire laser (120×450 nm) at different optical pump power densities. (b) The peak intensity curve of the Sample A GaN nanowire laser versus pump power density and pump fluence (L-L curve). The pump laser has a pulse width of 400 ps. The L-L curve indicates a lasing threshold of ~440 kW/cm^2 (~176 μJ/cm^2).

The μ-PL spectra of an as-fabricated GaN nanowire laser (Sample A) are plotted in Figure 2(a) for several pump power levels. At lower powers, because the spontaneous emission with random photon state is stronger than the stimulated emission, a ~7.4 nm wide broad-band spectrum centered at 364.7 nm was observed. When the nanowire was optically pumped at ~682 kW/cm^2, stimulated emission becomes dominant. The GaN nanowire optical cavity then provided the wavelength selection mechanism. Therefore, a narrow-band lasing peak

6

centered at 363 nm with full width half maximum (FWHM) of 0.16 nm was observed. Another broader peak centered at 365 nm with a FWHM of 0.39 nm was also observed possibly corresponding to amplified spontaneous emission.[27] The peak intensity of the spectra is plotted as a function of pump power density (Figure 2(b)). When the nanowire laser was pumped above the lasing threshold, the non-radiative recombination rate is clamped due to the saturated carrier density. The clear slope change in the light-light (L-L) curve from low pump power density to high pump power density indicates a transition to lasing behavior. The lasing threshold was estimated as ~440 kW/cm^2 (~176 μJ/cm^2) by fitting the peak intensities after the slope change with a linear function of the pump power density.

(a)

(b)
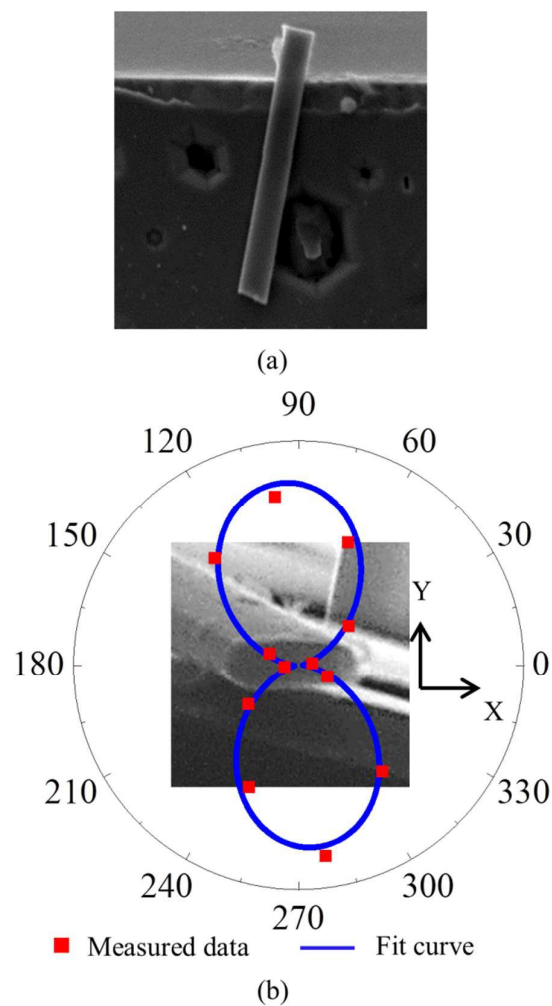
Figure 3. (a) SEM image of a rectangular GaN nanowire laser (Sample A) hanging off a edge of a sapphire substrate. (b) Peak intensity of the end-facet emission from the nanowire laser plotted as a function of polarization angle, demonstrating linearly polarized emission with an extinction ratio of 14:1. Inset: the SEM image of the GaN nanowire partially hanging off the edge of the substrate. The major axis of the linearly polarized emission is along the y-direction of the rectangular nanowire laser.

The polarization of the end-facet lasing emission from a rectangular GaN nanowire laser (Sample A) hanging off an edge of a sapphire wafer was measured using the collection arm of the μ-PL system. The peak intensity of the lasing peak is plotted as a function of the angle θ of the analyzing polarizer (Figure 3). The peak intensity reached a maxima at $\theta = 95°$ and decreased to nearly 0 at $\theta = 5$, giving an extinction ratio of approximately 14:1. The "figure-eight" shaped curve indicates a linearly polarized emission from the GaN nanowire laser oriented along the short dimension (y-dimension) of the rectangular cross-section. The measurement was repeated with 3 other Sample A nanowires, confirming linear polarization along the y-dimension of the rectangular cross-sections, with extinction ratios of 44:1, 30:1, and 13:1, respectively. In contrast, previous work has demonstrated that the emission from c-axis oriented cylindrical GaN nanowire lasers are elliptically polarized with random orientation of the major axis of the polarization with respect to the underlying substrate[22,26].
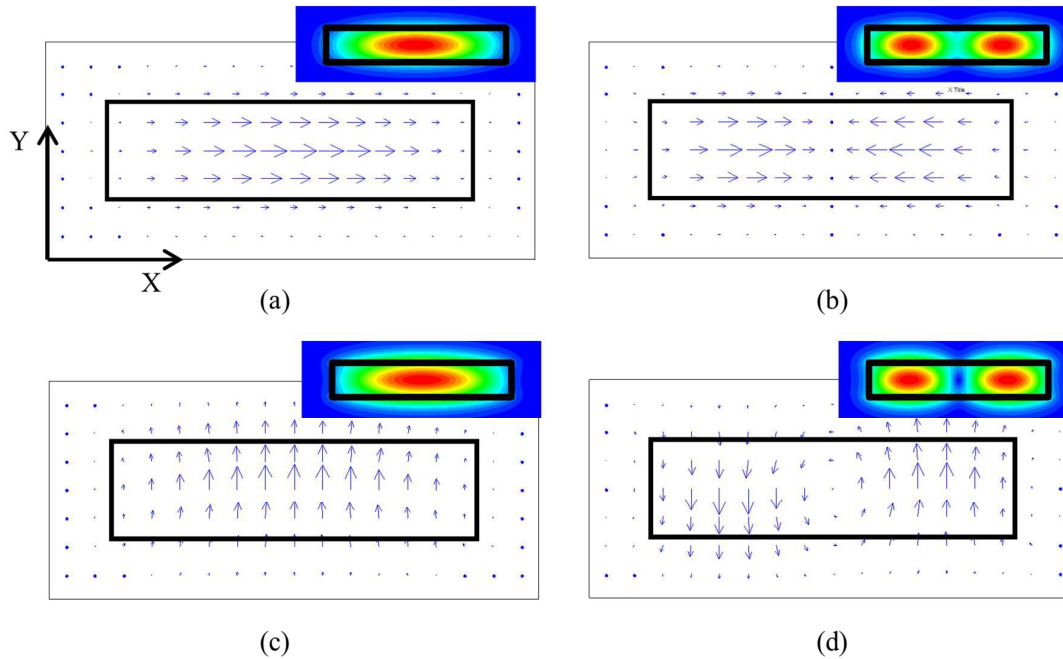
Figure 4. Electric fields of the first 4 transverse modes (a-d) supported by a GaN nanowire laser with rectangular cross-section. (a) and (b) correspond to the x-polarized modes. (c) and (d) correspond to the y-polarized modes. The vectors represent the directions and magnitudes of the electric fields. Insets: Intensities of electric fields for the corresponding modes. The black boxes represent the rectangular (120×450 nm) GaN nanowire cross-section. The electrical fields are linearly polarized with extinction ratios of > 32:1.

In order to study the mechanism of linear polarization, an eigenmode solver (MODE solutions from Lumerical Inc.[28]) was utilized to simulate the transverse modes supported by a waveguide with a rectangular cross-section. The waveguide, matching the geometry of Sample A with a cross-sectional x-dimension of 450 nm and y-dimension of 120 nm, was placed at the center of the simulation model. The refractive index of a *c*-plane GaN epitaxial film grown on sapphire was measured by ellipsometry and used in the simulation. In order to eliminate the influence from the boundary of the simulation, the boundary was set as a perfectly matched layer. A mesh size of 1 nm was used to ensure sufficient accuracy of the

simulation. The simulation shows that, unlike traditional cylindrical nanowires, well confined

transverse modes supported by the rectangular waveguide are linearly polarized (Figure 4).

Because the optical modes have different volumes than the gain medium of a nanowire, only

the portion of an optical mode that overlaps the gain medium obtains the optical gain (known

as the modal gain). The modal gain $\langle g \rangle$ of the transverse modes of the rectangular nanowire

lasers is given by:

$$\langle g \rangle = \Gamma_{xy} \Gamma_z g \tag{2}$$

Where Γ_z and g are the longitudinal confinement factor and the material gain, respectively.

It is reasonable to assume that Γ_z and g are constant, because the nanowires are uniformly

pumped, and the GaN material quality is assumed to be uniform throughout the nanowire.

Therefore, the modal gain is proportional to the transverse confinement factor.

The transverse confinement factor Γ_{xy} for a rectangular cross-sectioned nanowire is given

by[29]:

$$\Gamma_{xy} = \frac{n}{\bar{n}} \times \frac{\int_{-w2/2}^{w/2} \int_{-d/2}^{d/2} |U(x,y)|^2 dxdy}{\iint_{xy} |U(x,y)|^2 dxdy} \tag{1}$$

Where w, d, n are the x-dimension, y-dimension, and refractive index of the rectangular

nanowire, respectively, and $\bar{n}$ is the effective refractive index of a transverse mode. The

second term represents the ratio of the electromagnetic field amplitude inside of the nanowire

to the total electromagnetic field amplitude.

Simulation results of the transverse confinement factors for the first 3 x-polarized modes

(X1~X3) and the first 3 y-polarized modes (Y1~Y3) are plotted in logit scale in Figure 5. Consistent with previous research[24], the simulation results show that when the y-dimension is below ~55 nm (Region I), the modes with a polarization along the y-direction are not well-confined, resulting in only transverse modes with x-polarization. Due to the difficulty of fabrication, the minimum y-dimensions of our fabricated GaN nanowires are ~120 nm (Region II). In this case, the second terms in equation (1) for x-polarized and y-polarized modes are closer in magnitude. Meanwhile, the rectangular cross-section of the GaN nanowire results in lower $\bar{n}$ for y-polarized modes than for x-polarized modes, leading to a higher confinement factor for y-polarized modes. Thus, according to equation (2), y-polarized modes should have higher modal gain than x-polarized modes in Region II. Although the mode confinement contrast is not as large as in Region I, it is still sufficient to provide the mode selection mechanism, due to the mode competition process in a laser.
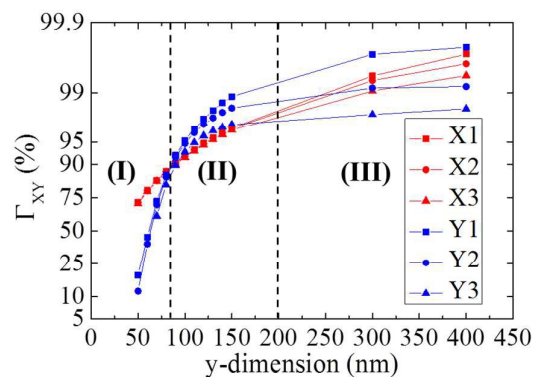
Figure 5. (a) Simulation results for the transverse confinement factors for the first 3 x-polarized modes (X1~X3) and the first 3 y-polarized modes (Y1~Y3) plotted in logit scale.

In order to verify the simulation results, rectangular nanowires with a reduced cross-sectional anisotropy (Sample B, x = 450 nm, y = 300 nm) were also optically pumped. Due to the more

similar transverse confinement factors for x-polarized and y-polarized modes, elliptically

polarized, rather than linearly polarized, lasing was observed with extinction ratios of 2.8:1,

7.1:1, 3.1:1, 1.2:1 and 8.1:1 (Figure 6(b)). Thus, this result is consistent with the predicted

elliptical polarization for nanowires with dimensions corresponding to Region III in Figure 5.
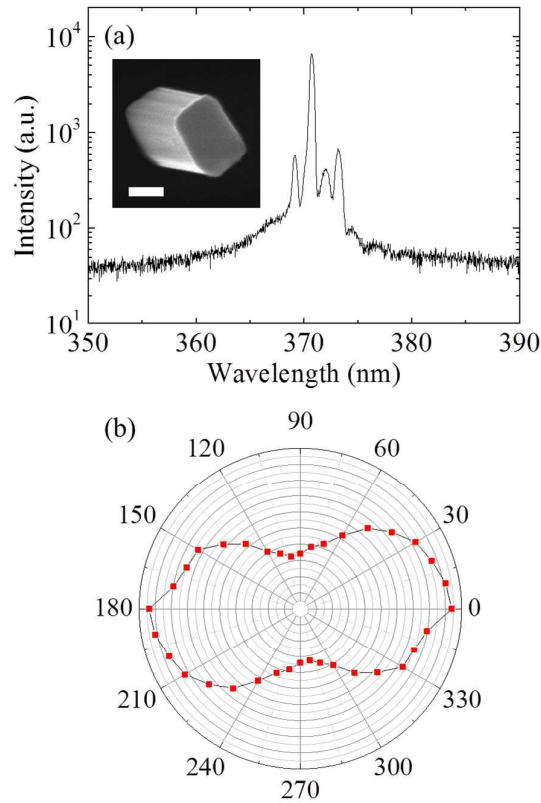
Figure 6. (a) Lasing spectrum of the emission from a Sample B GaN nanowire laser with a

y-dimension of 300 nm (compared to y~120 nm for Sample A). Inset shows the SEM image

of the Sample B GaN nanowire hanging off the cleaved edge of a silicon substrate. Scale bar:

200 nm (b) Peak intensity of the end-facet emission as a function of the polarization angle.

The results show an elliptically polarized lasing emission with an extinction ratio of 2.8:1.

Conclusions

In conclusion, by using a top-down two-step dry plus wet etching process, GaN nanowire

with rectangular cross-sections and exhibiting inherent, linearly polarized lasing were

demonstrated. The rectangular cross-section breaks the mode degeneracy for x-polarized and y-polarized modes, resulting in higher confinement factor and higher modal gain for the y-polarized modes. Consequently, intrinsic, linearly polarized lasing emission oriented along the short y-direction from rectangular cross-sectioned GaN nanowire lasers was consistently observed under optical pumping. More generally, these results demonstrate that cross-sectional control offers the ability to inherently control the polarization from individual nanowire lasers without additional environmental requirements such as placement onto lossy substrates, which will greatly broaden their potential application space. For example, intrinsic, linearly polarized nanowire lasers can be transferred to photonic integrated circuit platforms to simplify the polarization-independent design of functional building blocks, such as directional couplers or ring resonators, which is not trivial and sometimes even impossible[30].

Corresponding Author

*E-mail: gtwang@sandia.gov

managed and operated by Sandia Corporation, a wholly owned subsidiary of Lockheed Martin Corporation, for the U.S. Department of Energy's National Nuclear Security Administration under contract DE-AC04-94AL85000.

References

1 M. Law, D. J. Sirbuly, J. C. Johnson, J. Goldberger, R. J. Saykally and P. Yang, *Science*, 2004, **305**, 1269–1274.

2 Y. Ma, X. Guo, X. Wu, L. Dai and L. Tong, *Adv. Opt. Photonics*, 2013, **5**, 216–273.

3 D. J. Sirbuly, M. Law, P. Pauzauskie, H. Yan, A. V Maslov, K. Knutsen, C. Ning, R. J. Saykally and P. Yang, *Proc. Natl. Acad. Sci. U. S. A.*, 2015, **102**, 7800–7805.

4 Q. Li, J. B. Wright, W. W. Chow, T. S. Luk, I. Brener, L. F. Lester and G. T. Wang, *Opt. Express*, 2012, **20**, 17873–17879.

5 H. Xu, J. B. Wright, T.-S. Luk, J. J. Figiel, K. Cross, L. F. Lester, G. Balakrishnan, G. T. Wang, I. Brener and Q. Li, *Appl. Phys. Lett.*, 2012, **101**, 113106.

6 H. Gao, A. Fu, S. C. Andrews and P. Yang, *Proc. Natl. Acad. Sci. U. S. A.*, 2013, **110**, 865–869.

7 Y. Xiao, C. Meng, P. Wang, Y. Ye, H. Yu, S. Wang, F. Gu, L. Dai and L. Tong, *Nano Lett.*, 2011, **11**, 1122–1126.

8 J. B. Wright, S. Campione, S. Liu, J. a. Martinez, H. Xu, T. S. Luk, Q. Li, G. T. Wang, B. S. Swartzentruber, L. F. Lester and I. Brener, *Appl. Phys. Lett.*, 2014, **104**, 041107.

9 H. Xu, J. B. Wright, A. Hurtado, Q. Li, T.-S. Luk, J. J. Figiel, K. Cross, G. Balakrishnan, L. F. Lester, I. Brener and G. T. Wang, *Appl. Phys. Lett.*, 2012, **101**, 221114.

10 J. B. Wright, S. Liu, G. T. Wang, Q. Li, A. Benz, D. D. Koleske, P. Lu, H. Xu, L. Lester, T. S. Luk, I. Brener and G. Subramania, *Sci. Rep.*, 2013, **3**, 2982.

11 S. Ishizawa, K. Kishino, R. Araki, A. Kikuchi and S. Sugimoto, *Appl. Phys. Express*, 2011, **4**, 055001.

12 A. Pan, W. Zhou, E. S. P. Leong, R. Liu, A. H. Chin, B. Zou and C. Z. Ning, *Nano Lett.*, 2009, **9**, 784–788.

13 F. Qian, Y. Li, S. Gradecak, H.-G. Park, Y. Dong, Y. Ding, Z. L. Wang and C. M. Lieber, *Nat. Mater.*, 2008, **7**, 701–706.

14 Z. Yang, D. Wang, C. Meng, Z. Wu, Y. Wang, L. Dai, X. Liu, X. Liu and Q. Yang, *Nano Lett.*, 2014, **14**, 3153–3159.

15 X. Liu, Q. Zhang, Q. Xiong and T. C. Sum, *Nano Lett.*, 2013, **13**, 1080–1085.

16 X. Liu, Q. Zhang, J. N. Yip, Q. Xiong and T. C. Sum, *Nano Lett.*, 2013, **13**, 5336–5343.

17   S. Liu, C. Li, J. J. Figiel, S. R. J. Brueck, I. Brener and G. T. Wang, *Nanoscale*, 2015, **7**, 9581–9588.

18   C. Li, S. Liu, A. Hurtado, J. B. Wright, H. Xu, T. S. Luk, J. J. Figiel, I. Brener, S. R. J. Brueck and G. T. Wang, *ACS Photonics*, 2015, **2**, 1025–1029.

19   T. Okoshi, *J. Light. Technol.*, 1985, **3**, 1232–1237.

20   J. Noda, K. Okamoto and Y. Sasaki, *J. Light. Technol.*, 1986, **4**, 1071–1089.

21   J. C. Johnson, H. Yan, R. D. Schaller, P. B. Petersen, P. Yang and R. J. Saykally, *Nano Lett.*, 2002, **2**, 279–283.

22   H. Xu, A. Hurtado, J. B. Wright, C. Li, S. Liu, J. Figiel, T. Luk, S. R. J. Brueck, I. Brener, G. Balakrishnan, Q. Li and G. T. Wang, *Opt. Express*, 2014, **22**, 19198–19203.

23   M. Munsch, J. Claudon, J. Bleuse, N. S. Malik, E. Dupuy, J.-M. Gérard, Y. Chen, N. Gregersen and J. Mørk, *Phys. Rev. Lett.*, 2012, **108**, 077405.

24   A. P. Foster, J. P. Bradley, K. Gardner, A. B. Krysa, B. Royall, M. S. Skolnick and L. R. Wilson, *Nano Lett.*, 2015, **15**, 1559–1563.

25   Q. Li, K. R. Westlake, M. H. Crawford, S. R. Lee, D. D. Koleske, J. J. Figiel, K. C. Cross, S. Fathololoumi, Z. Mi and G. T. Wang, *Opt. Express*, 2011, **19**, 25528–25534.

26   A. Hurtado, H. Xu, J. B. Wright, S. Liu, Q. Li, G. T. Wang, T. S. Luk, J. J. Figiel, K. Cross, G. Balakrishnan, L. F. Lester and I. Brener, *Appl. Phys. Lett.*, 2013, **103**, 251107.

27   M. a. Zimmler, J. Bao, F. Capasso, S. Müller and C. Ronning, *Appl. Phys. Lett.*, 2008, **93**, 051101.

28   Lumerical Solutions, Inc. http://www.lumerical.com/tcad-products/mode/

29   L. A. Coldren and S. W. Corzine, *Diode Lasers and Photonic Integrated Circuits*, Wiley, 2nd edn., 2012.

30   G. T. Reed, G. Z. Mashanovich, W. R. Headley, B. Timotijevic, F. Y. Gardes, S. P. Chan, P. Waugh, N. G. Emerson, C. E. Png, M. J. Paniccia, A. Liu, D. Hak and V. M. N. Passaro, *IEEE J. Sel. Top. Quantum Electron.*, 2006, **12**, 1335–1343.